CORA Cork Open Research Archive
Cartlann Taighde Oscailte Chorcaí

Title	Nanoporous gold anode catalyst for direct borohydride fuel cell
Authors	Nagle, Lorraine C.;Rohan, James F.
Publication date	2011-08-01
Original Citation	Nagle, Lorraine C.,Rohan, James F. (2011) 'Nanoporous gold anode catalyst for direct borohydride fuel cell'. International Journal of Hydrogen Energy, 36 (1616):10319-10326.
Type of publication	Article (peer-reviewed)
Link to publisher's version	http://www.sciencedirect.com/science/article/pii/S0360319910019841 - 10.1016/j.ijhydene.2010.09.077
Rights	NOTICE: this is the author's version of a work that was accepted for publication in International Journal of Hydrogen Energy. Changes resulting from the publishing process, such as peer review, editing, corrections, structural formatting, and other quality control mechanisms may not be reflected in this document. Changes may have been made to this work since it was submitted for publication. A definitive version was subsequently published in International Journal of Hydrogen Energy, [Volume 36, Issue 16, August 2011] DOI: http://dx.doi.org/10.1016/j.ijhydene.2010.09.077 - https://creativecommons.org/licenses/by-nc-nd/4.0/
Download date	2026-11-07 05:15:26
Item downloaded from	https://hdl.handle.net/10468/1072

UCC
University College Cork, Ireland
Coláiste na hOllscoile Corcaigh

Nanoporous gold anode catalyst for direct borohydride fuel cell

Lorraine C. Nagle* and James F. Rohan
Tyndall National Institute, Lee Maltings, Prospect Row, Cork, Ireland.

*Corresponding author
Tel +353 21 4904266
Fax +353 21 4904058
E-mail address lorraine.nagle@tyndall.ie

Abstract
Nanoporous gold (NPG) electrodes were fabricated in film and wire array formats by selectively dealloying Ag from $Au_{0.18}Ag_{0.82}$. Borohydride oxidation reaction (BOR) was studied by cyclic voltammetry at the NPG electrodes. The onset potential for the oxidation at a NPG wire array shifted to more negative potentials that than observed at a Au disc and higher currents were realised. An onset potential of -1.07 V vs. Ag/AgCl which is 0.207 V lower than that at a Au disc was recorded. The oxidation current for 20 mM borohydride in 1 M NaOH increased to 73.6 mA cm^{-2} from 3.17 at a Au disc. A value of 7.49 electrons was determined for n out of a possible 8 for borohydride oxidation. NPG presents an attractive alternative to gold nanoparticle-based catalysts for use in direct borohydride fuel cells. NPG can establish intimate contact with an electrical substrate and eliminates the need for a carbon support.

Keywords
Borohydride
Gold
Nanoporous gold
Direct Borohydride fuel cell

1. Introduction
Direct Borohydride Fuel Cells (DBFCs) are currently under investigation in an effort to develop sustainable power sources. Their target specification of 600–1000 Wh kg^{-1} is 5-6 times the energy density of lithium-ion batteries. The DBFC system was first proposed in the 1960s: Indig and Snyder reported a practical demonstration of direct electricity generation from borohydride ions [1]. Research on DBFC technology stagnated then until the late 1990s. Amendola et al. reported on the performance of a DBFC system using Au–Pt alloy electroplated on carbon cloth as the anode [2]. Following further impressive research efforts over the next 5 years the first demonstration of a DBFC system for laptop computers was presented in 2005 by the Materials and Energy Research Institute (MERIT) who succeeded in increasing the DBFC system output from 10 to 400 W [3]. Recent vigorous research on DBFCs has greatly raised the expectation for the realization of the various benefits promised by this fuel cell system for portable applications [4]. Establishing the technology requires an understanding of the mechanism of borohydride oxidation and its associated catalytic species. The DBFC decomposes and oxidizes the fuel directly,

Cathode: $2O_2 + 4H_2O + 8e^- \Rightarrow 8OH^-$ $E^0 = 0.40$ V (1)

Anode: $NaBH_4 + 8OH^- \Rightarrow NaBO_2 + 6H_2O + 8e^-$ $E^0 = 1.24$V (2)

The equilibrium voltage, $E^0 = 1.64$ V, compares favourably with DMFC and H_2/O_2 fuel cells that have equilibrium voltages of 1.21 V and 1.24 V, respectively. Borohydride is

a promising fuel given its high theoretical specific energy, high specific capacity and good anode performance. Careful selection of the anode catalyst is crucial in minimising competing borohydride hydrolysis given by Eqns. 3 and 4 which can result in heterogeneous, non-faradaic hydrogen evolution that decreases fuel utilisation and lowers cell performance,

$BH_4^- + H_2O \Rightarrow BO_2^- + H_2$ (3)
$BH_3OH^- + H_2O \Rightarrow BO_2^- + 3H_2$ (4)

In practice the actual anodic reaction depends on the ratio of hydroxide to borohyride ion and is more realistically represented by Eqn. 5
$BH_4^- + nOH^- \Rightarrow BO_2^- + (n-2)\ H_2O + ne + (4-0.5\ n)\ H_2$ (5)

New ref for this Eqn.5 from IJHE to add here
Concentration ratio of [OHL]/[BH4L]: A controlling factor for the fuel efficiency of borohydride electro-oxidation
Bin Hong Liu a, Jun Qiang Yang a, Zhou Peng Li
I n t e r n a t i onal j o u r n a l o f hydrogen energy 3 4 (2 0 0 9) 3 3 6 0 – 3 3 6 6

Earlier it was believed that the platinum group metals show poor faradaic efficiency for borohydride oxidation while gold was believed to be an effective catalyst for borohydride oxidation and non-catalytic with regard to its hydrolysis regarded. The oxidation of borohydride and its hydrolysis product, BH_3OH^- has been studied extensively at a range Au electrodes [5- adjust]. It was shown recently that gold does in fact show catalytic activity for hydrolysis of BH_4^- and BH_3OH^- [9, 10].

New ref for to add here
M. Chatenet, F. H. B. Lima, E. A. Ticianelli, J. Electrochem. Soc., 157 (2010) B697.

The faradaic efficiency of gold for borohydride oxidation has been shown to be lower than that assumed previously [11 and above new ref]. Gold does in fact catalyse BH_4^- and BH3OH− hydrolysis to produce H2. Chatenet [above new ref] showed that by coupling online MS with electrochemistry evidence of H2 formation during oxidation of BH_4^- on Au could be obtained. This originated from the partial hydrolysis of BH4 − into BH3OH−. They observed the onset of faradaic BH4− oxidation coincided with H2 evolution and this increases monotonically with electrode potential up to 0.8 V vs RHE (ca. -0.2 V SCE) until it reaches ca. 6.5–7.4 electrons per BH4− species for 0.1 M NaBH4 and 0.015 or 0.003 M NaBH4, respectively in the high potential region. Their proposed pathway assumes the generation of BH3OH− and H2 at low potential, followed by the oxidation of BH3OH− when these species can remain long enough at the vicinity of the electrode surface. At higher potential, the direct and complete BOR becomes more likely, yielding to a rather high faradaic efficiency. In a RDE analysis of BH_4^- oxidation Finkelstein [11] showed that the electron count, n, for the reaction is potential dependent. They identified two regions of mass transport limited current from -0.45 to -0.35 V and -0.20 to +0.28 V vs Ag/AgCl. Levich analysis showed that the higher potential wave yields 7 e per molecule while the lower potential wave yields 4.5 e. In our study a n value of 7.49 at the oxidation plateau centered at 0.0 V vs SCE was determined which is in agreement with the findings of Chatenet and Finkelstein [11 and above new ref].

It was just recently shown that the platinum can show high catalytic activity for borohydride oxidation and low activity for its competing hydrolysis under certain conditions and may yield nearly 8 electrons per BH4- species. For smooth Pt Finkelstein et al [11] demonstrated that the direct oxidation of borohydride at low potentials (-0.8 to -0.25 V vs Ag/AgCl) yields 7 electrons and requires the presence of Pt surface hydrides. Molina Concha et Chatenet [ref 2 from Reviewer 2] showed that for carbon-supported platinum catalysts a n value of almost 8 has been obtained for a certain active catalyst layer thickness. This was explained in terms of an increased residence time of H_2 formed by hydrolysis and BOR intermediates within the layer to favour the complete BOR and/or hydrogen oxidation.

[ref 2 from Reviewer 2]
B. Molina Concha, M. Chatenet, Electrochim. Acta, 54 (2009) 6130.

NPG is an interconnected, bicontinuous ligament network containing regions of both negative and positive curvature which topologically requires a high step density. NPG can be formed by a **c**hemical etching process called dealloying which involves selective metal dissolution. Forty has shown that depletion gilding of a less-noble metal from Au alloys results in an open, continuous nanoporous structure composed of Au [16]. As the Ag atoms in an Ag_xAu_y alloy are dissolved in acid, remaining Au atoms gather together in clusters that create a rough surface causing Au to evolve into a porous material. The sponge-like 3D structure is a system of interconnecting pores/tunnels in a skeleton of filaments of the metal. The filament size can range from 5-50 nm with surface areas as high as 20 $m^2 g^{-1}$ and a porosity of 70 % or higher possible. Biener et al. [17] indicated that NPG brings together two seemingly conflicting properties: high strength and high porosity. They characterized the size-dependent mechanical properties of NPG using a combination of nanoindentation, column microcompression, and molecular dynamics simulations. It was shown that NPG can be as strong as bulk Au, despite being a highly porous material and that its ligaments approach the theoretical yield strength of Au. Structurally it bears a resemblance to naturally occurring zeolites (filament size 1-2 nm and surface areas 100 $m^2 g^{-1}$) [18].

This useful but relatively unstudied form of Au most likely contains an intrinsically high step density which makes it attractive for catalysis studies. It is even more attractive because it can be formed into thin, high-conductivity foils that are easily adapted to electrocatalytic measurements. In terms of catalytic applications, NPG has at least two advantages over other catalysts or Au nanoparticles. Firstly, NPG remains active at low temperature (room temperature or even lower), unlike Pt or Pd catalysts [21 and Topics in Catal below]. Research has suggested that gold nanoparticle based catalysts can display low temperature activity and selectivity under a range of conditions relevant to automotive pollution control. [Topics in Catal below].

New ref to add
Topics in Catalysis Vols. 30/31, July 2004
The potential for use of gold in automotive pollution control technologies: a short review
G. Pattricka, E. van der Lingena, C.W. Cortib, R.J. Holliday,b,* and D.T. Thompsonb

Platinum group metals (PGMs) are currently used for both anode and cathode catalysts in most commercial proton exchange membrane fuel cells (PEM). The tendency for poisoning of platinum by CO contaminant in the hydrogen feedstock gas remains a major technical hurdle.
Gold was shown to have particularly good catalytic performance for the oxidation of carbon monoxide. However, compared to research focused on the use of PGMs for automotive pollution control, the science of gold catalysis is still in it's infancy.

Stable low temperature CO oxidation over unsupported NPG was shown by Xu et al. [21]. A significant CO conversion rate at -30oC was sustained for longer times that that recorded at room temperature. The room temperature deactivation originated from an increase in ligament size which resulted in pore clogging and a decrease in active surface area. Secondly, NPG exhibits good thermal stability and resistance to oxidation [19] and thus can overcome the aggregation or sintering limitations which Au nanoparticles encounter at elevated temperatures or in an oxidative environment [20]. NPG in a foam type structure has been shown to exhibit high CO oxidation activity, however, the catalytic reactions only occur at the foam surface [22]. Zeis et al. [23] demonstrated that NPG is an effective catalyst for the reduction of hydrogen peroxide to water. The reaction efficiency is sufficiently high to allow use of the material as a cathode for oxygen reduction in hydrogen PEM fuel cells, although the overall efficiency in this context is still far less efficient than that of Pt. Their results are consistent with their overall hypothesis that the central difference between NPG and bulk Au is due to the increased density of step edges in NPG over bulk Au. In summary, using nanoporous metal electrodes for fuel cell electrodes opens exciting new avenues for catalyst design.

In this paper we report on the exploitation of nanoporous gold (NPG) with high specific surface area and electrocatalytic activity to develop an anode catalyst with high catalytic activity for oxidation of borohydride and low activity for its competing hydrolysis.

2. Materials and methods

2.1 Materials used

Sodium borohydride (minimum purity 98 %), sodium carbonate (minimum purity 99%) and sodium hydroxide, NaOH (minimum purity 99%) were purchased from Sigma Aldrich and used as received. $KAg(CN)_2$ (minimum purity 99%) and $KAu(CN)_2$ (minimum purity 99%) were purchased from Johnson Matthey and used as received. Anodisc alumina circular membranes (Anodisc® 25) 2.5cm in diameter, 60 micron thick, 200 nm pore size and 10^9 pore openings per cm^2 of membrane were supplied by Whatman™. These show compatibility with a wide range of solvents and acids and can be dissolved in sodium hydroxide and ammonium hydroxide solutions. The maximum temperature at which they are stable is 400°C. Deionized water of resistivity 18 MΩ cm was used to prepare all solutions. The working electrodes was 5 mm Au disc (Princeton Applied Research) supplied by Advanced Measurement Technology, U.K. These were polished with 0.5μm alumina powder obtained from Struers on a Buehler polishing cloth for 2 minutes and rinsed in deionized water. A 1 mm diameter Au counter electrode of 50 mm length was used.

2.2 Electrochemical measurements

Cyclic voltammograms (CV) were recorded with respect to a standard calomel electrode. The potential of the working electrode was controlled using a CH Instruments potentiostat model 660B with picoamp booster. All solutions were purged with nitrogen for 20 min prior to experiments in order to remove oxygen, and the experiments were performed at room temperature.

2.3 Fabrication of NPG

Ag_xAu_y films were deposited on a 200 nm Au film on pyrex at constant potential of -1.2 V from a solution of 100 mM $KAg(CN)_2$ and 20 mM $KAu(CN)_2$ in 250 mM Na_2CO_3, pH 13 for 5000 s. EDX confirmed that an alloy composition of $Au_{0.18}Ag_{0.82}$ was formed. It was demonstrated by Searson et. al [24] that the morphology and porous structure of NPG depends on the composition of the Ag_xAu_y alloy for the range $0.18 \leq x \geq 0.32$. The alloy composition $Au_{0.18}Ag_{0.82}$ gives the highest surface area NPG (6.9 m^2 g^{-1}) when dealloyed in nitric acid and the shortest ligament size of 20-30 nm. The CV response recorded for the alloy in 1 M NaOH from -0.9 to 0.6 V vs. SCE at 10 mV s^{-1} (not shown here) indicated the presence of Au and Ag from the metal oxide reduction peaks seen at -0.1 V and 0.4 V, respectively. Upon immersing the $Au_{0.18}Ag_{0.82}$ in 30 % nitric acid for 15 min a high surface area form of Au referred to as NPG is obtained. The thickness of NPG was measured as 2 micron using SEM. The NPG film was delaminated from the underlying Au film and sandwiched in a holey Cu folding TEM grid in order to obtain the TEM image shown in Fig. 1. The pore and ligament size are 20 nm and 30 nm, respectively.

The fabrication of NPG on a Au disc was achieved using the conditions given above for the fabrication of NPG on a planar Au film. The fabrication of a NPG in a 3D wire array format was achieved by dealloying Ag_xAu_y nanowires that were deposited in Anodisc alumina membranes with 200 nm pore size using the conditions given above for the fabrication of NPG on a planar Au film. The alumina membrane had a conducting backing layer of 350 nm Au which was sputter deposited. The alumina was dissolved by soaking it in 0.5 M NaOH for 2 hours to release the NPG wires. The SEM image shown in Fig.2 was recorded for the resulting NPG wires.

The fabrication of a segmented NPG-Au wire array was demonstrated to add structural rigidity to the NPG wire array. A 3D Au wire array was deposited from a commercial Puramet bath in Anodisc alumina membranes with a 350 nm Au conducting backing layer which was sputter deposited. The Au wires were deposited to a length of 3 micron and 200 nm in diameter. The fabrication of NPG onto the Au wires was achieved by dealloying Ag_xAu_y wires that were then deposited on the Au wires in the Anodisc alumina membranes using the conditions given above for the fabrication of NPG on a planar Au film. The alumina was dissolved by soaking it in 0.5 M NaOH for 2 hours to release the segmented Au-NPG wires. The SEM image shown in Fig. 3 was recorded for the resulting segmented NPG-Au 3D wire array.

2.4 Characterisation of NPG

TEM images were recorded using JEOL 2000FX at an accelerating voltage of 200 kV. SEM images were recorded using Nova Nanosem 630 at an accelerating voltage of 15 kV

3. Results and discussion

3.1 Cyclic voltammetry study

Cyclic voltammograms for a Au disc, NPG on the Au disc, NPG-Au segmented wire array and NPG wire array in 1 M NaOH are shown in Figure 4. They clearly illustrate the influence of the increased surface area of the electrodes. The oxidation response for 0.02 mM $NaBH_4$ in 1 M NaOH at a Au disc and NPG-coated Au disc under static conditions is shown in Fig. 5. The onset of oxidation at the Au disc is -0.80V and oxidation is sustained at the gold surface until 0.05 V when gold oxides form which are inactive for BH_4^- oxidation. In the subsequent reverse sweep the oxidation recommences at 0.10 V upon gold oxide reduction. The onset of BH_4^- oxidation at the NPG-coated Au disc has shifted to -0.97 V. The peak a1 at -0.49 V has been reported previously in the literature [6,7,9] and has–been assigned to the oxidation of a species in solution as shown by Chatenet at al [9] and can be attributed to a combination of H2 oxidation and the low potential oxidation of BH4- [9, 11] The broad oxidation wave from -0.4 to 0.25 V may be ascribed to the high-potential oxidation of BH4- [9] and has been shown to correspond to the oxidation of adsorbed BH4- species. The oxidation of BH2(OH)2- was noted [9] to occur at 0.30 V. The oxidation of BH_4^- is sustained into the region of gold oxide formation indicating higher activity for the reaction than at the clean Au disc over this potential region. The BH_4^- oxidation current at the plateau centered at 0.0 V has increased from 3.17 at the Au disc to 38 mA cm^{-2} at the Au disc with NPG deposit.

3.2 Determination of n

The influence of scan rate on the oxidation response for borohydride was studied at the NPG-coated Au disc. The positive shift of the peak potential for a1, $E_{p\ a1}$, with increasing scan rate as shown in Fig. 6 is indicative of a sluggish reaction. The a1 peak current, $I_{p\ a1}$ increases linearly with the square root of scan rate as shown in Figure 7, this suggests that a1 can be attributed to the oxidation of a species in solution and there is no interference from adsorption. Using the Randles-Sevcik Equation 6 and Equation 7 the number of electrons, n, associated with a1 was calculated as 4.26.

$$Ip = 2.99\times10^{5}\alpha^{1/2}n^{3/2}CD^{1/2}\nu^{1/2} \quad (6)$$

$$n\alpha = \frac{1.857RT}{F(Ep - Ep_{0.5})} \quad (7)$$

The n value obtained indicates the direct oxidation of BH_4^- is incomplete at -0.49 V and its oxidation product is oxidised at more positive potentials.

The influence of rotation rate on the oxidation response $NaBH_4$ was studied at the NPG-coated Au disc, as is shown in Fig. 8. Levich analysis using equation 8 shown in Fig.10 of the oxidation plateau at 0.0 V revealed a diffusion-controlled reaction and the attainment of near-maximum coulombic efficiency for borohydride oxidation with n=7.49.

$$I_{lim} = 0.62nFCD^{2/3}\nu^{-1/6}\Omega^{1/2} \quad (8)$$

where the kinematic viscosity (ν) = 1.14×10^{-2} cm^2 s^{-1} and the diffusion coefficient (D) = 1.28×10^{-5} cm^2 s^{-1}.

The values used for D and ν were those recently determined by Chatenet et al (new ref to add below)for 10 mM NaBH4 in 1 M NaOH at 25^{o}C.

New ref to add
M. Chatenet, M. B. Molina-Concha, N. El-Kissi, G. Parrour, J.-P. Diard, Electrochim. Acta, 54 (2009) 4426.

The n values determined here support those recently determined in a RDE study of BH_4^- oxidation at Au by Finkelstein et. al [11] where they reported that a 7-8 e oxidation of BH_4^- occurs at -0.2 V vs. Ag/AgCl and that the oxidation peak at -0.52 V vs. Ag/AgCl yields 4.5 electrons per molecule with the remainder of the electrons possibly generating hydrogen.

3.3 Linear sweep voltammetry study

The linear sweep voltammograms for the oxidation of borohydride at the fabricated electrodes is compared in Fig. 10. The current for the oxidation of 20 mM borohydride at the Au disc, Au disc with NPG deposit and NPG wire array at the plateau centered at 0.0 V was measured as 3.17, 25, 38 and 73.6 mA cm^{-2}, respectively. The geometrical area exposed to the electrolyte was used to calculate the current density for each electrode. This equates to a 8-, 12- and 24-fold increase in current at the segmented Au-NPG wire array, Au disc with NPG deposit and NPG wire array, respectively over that recorded at the Au disc. The onset potential for borohydride oxidation shifts from -0.80 V at the Au disc to -0.87 V, -0.95 and -1.07 V at the segmented NPG-Au wire array, Au disc with NPG deposit and NPG wire array, respectively. The increased density of active sites at NPG over smooth gold may account for the lower onset potential for BOR. It was also shown by Chatenet et al that the onset for BOR is lower at carbon supported gold nanoparticles (-0.57 V vs NHE) than at bulk gold (-0.50V vs NHE).
New ref to add here:
Electrochim acta 2006
Kinetics of sodium borohydride direct oxidation and oxygen reduction insodium hydroxide electrolyte Part I. BH4− electro-oxidation on Au and Ag catalysts
Marian Chatenet ∗ , Fabrice Micoud, Ivan Roche, Eric Chainet

The electrochemically surface areas of the three NPG were estimated from the charge associated with the gold oxide reduction peak in I M NaOH assuming that the charge/area ratio is usually considered to be ca. 400 μC cm^{-2} for a regular polycrystalline Au electrode. The real surface areas were calculated to be 610, 1009, 1240 cm^2 for the segmented NPG-Au 3D wire array, Au disc with NPG deposit and NPG wire array, respectively. The intrinsic electrode kinetic activity for the oxidation of 20 mM borohydride in 1M NaOH was calculated as 4.59, 7.52 and 72.1 μ A cm-2 for the segmented NPG-Au 3D wire array, Au disc with NPG deposit and NPG wire array, respectively. The intrinsic kinetic activity of the NPG electrodes cannot be compared with other gold-based electrodes from the literature as the electrochemically active surface areas for these are not given. The catalytic activity can only be compared to these electrodes based on the reported oxidation current densities based on the geometric electrode area. The reported oxidation current for 20 mM borohydride in 3M NaOH at 10 mVs-1 at a gold foil, ETEK 10 wt% gold on Vulcan XC72R and gold nanoparticles supported on titanate nanotubes was 4.5,15

and 10 mA cm-2 [13]. The reported oxidation current for 100 mM NaBH4 in 1M NaOH at 10 mVs-1 at carbon-supported gold hollow nanospheres was 57 mA cm-2. [12].
The oxidation current for 20 mM borohydride in 1 M NaOH reported herein is 25, 38 and 73.6 mA cm^{-2} at a segmented NPG-Au wire array, Au disc with NPG deposit and NPG wire array, respectively. This comparison serves to highlight the superior activity of NPG over other gold-based electrodes for borohydride oxidation.
The primary reason that NPG is more catalytically active than bulk planar gold for BOR is that the catalytic sites are often crystal surface defects. At such sites gold atoms with lower bond coordination numbers exist which may aid adsorption of reactants via electronic or steric interactions. NPG intrinsically has a high step density and hence a greater number of active sites than bulk planar gold. Also, it is possible that the structure of the active layer at NPG promotes an increase in the residence time of BOR reaction intermediates at the surface leaving more time for complete oxidation to borate. Such behaviour was recently reported by Chatenet for Pt and Pt/C electrodes [new refs below] and by Schneider et al. [new ref below] for the (multi-step) oxygen reduction reaction at arrays of Pt nanostructures at planar glassy carbon electrodes .

New refs to insert
B. Molina Concha, M. Chatenet, Electrochim. Acta, 54 (2009) 6119.
B. Molina Concha, M. Chatenet, Electrochim. Acta, 54 (2009) 6130.
A. Schneider, L. Colmenares, Y. E. Seidel, Z. Jusys, B. Wickman, B. Kasemo, R. J. Behm, Phys. Chem. Chem. Phys., 10 (2008) 1931.

4. Conclusions
Borohydride oxidation was studied by cyclic voltammetry at NPG in a range of structures. The onset potential for borohydride oxidation shifted to more negative potentials that than observed at bulk Au. The onset potential shifts from -0.80 V at a Au disc to -0.87, -0.95 and -1.07 V vs. Ag/AgCl at a segmented NPG-Au wire array, Au disc with NPG deposit and NPG wire array, respectively. The oxidation current for 20 mM borohydride in 1 M NaOH increased from 3.17 at a Au disc to 25, 38 and 73.6 mA cm^{-2} at a segmented NPG-Au wire array, Au disc with NPG deposit and NPG wire array, respectively. A value of 7.49 electrons was determined for n out of a possible 8 for borohydride oxidation.

NPG presents an attractive alternative to gold nanoparticle-based catalysts for fuel cells as it does not require a carbon support thereby removing the stability issues associated with these. NPG as a thin foil may be incorporated as a porous catalyst electrode as it is shapeable and has mechanical, thermal and chemical stability coupled to high catalytic activity. It has a dual functionality in that it can act as a current collector and as a catalyst. It provides a solution to the sintering problems that plague nanoparticle based catalysts and will allow for establishing more intimate contact with an electrical substrateThe porous structure promotes mass transport of reactant to the active sites and release of gaseous by-products. The diffusion of an electroactive species to Au nanoparticles on a high surface area carbon support is limited by the low degree of porosity of the carbon support. The role of catalyst support is a topic of continuous debate and different mechanisms have been proposed. The controversy arises from the fact that the supported Au catalyst is a composite system and its catalytic activity results from an interplay of pretreatment conditions, particle size, preparation method and choice of support. By eliminating the support

effect in free-standing NPG a deeper insight into the origin of the exceptional catalytic behaviour of Au in nanostructured form can be gained.
NPG can be easily integrated into PEM fuel cells. NPG may be integrated into nafion-based MEAs in conventional PEM fuel cells. An example of a PEM fuel cell using Pt modified NPG was given in J. Power Sources 165 2007, p 65 Zeis et al. Another advantage from incorporation of NPG over platinum into fuel cells would be the useful enhancement in electrical conductivity that could be derived, due to the lower electrical resistivity of gold compared to platinum.
However, from a cost viewpoint NPG may not rival supported gold nanoparticle based catalysts due to the energy used in it's production, the amount of silver lost in etching the precursor alloy and most importantly the significant amount of gold it constitutes.

Acknowledgement

This work is supported by EPA funding; it is part of a STRIVE fellowship entitled "Zero Carbon Emission Micro Fuel Cell Design"; Contract No. 2007-FS-ET-6-M5.

References

[1] Indig ME and Snyder RN. Sodium borohydride an interesting anodic fuel. J Electrochem Soc 1962;109:1104-1107.
[2] Amendola SC, Onnerud P, Kelly M, Petillo P, Sharp-Goldman SL. Binder M. A novel high power density borohydride air-cell. J Power Sources 1999;84:130-3.
[3] Chino S, Nagano K, Direct borohydride fuel cell technology for PCs. Fuel Cells Bull; 2005;1:9-10.
[4] Wee JH. Which type of fuel cell is more competitive for portable application:Direct methanol fuel cells or borohydride fuel cells? J Power Sources.2006;161:1-10.
[5] Hong Liu B, Yang JQ, Peng Li Z .Concentration ratio of [OHL]/[BH4L]: A controlling factor for the fuel efficiency of borohydride electro-oxidation. Int J Hydrogen Energy 2009;34:3360–3363.
[6] Gardiner JA, Collat JW. Polarography of the tetrahydroborate ion the effect of hydrolysis on the system. Inorg Chem 1965;4:1208–1212.
[7] Mirkin M V, Yang, H, Bard, AJ. Borohydride oxidation at gold electrode. J Electrochem Soc 1992;139:2212-17.
[8] Gyenge E. Electrooxidation of borohydride on gold and platinum electrodes:implications for direct borohydride fuel cells. Electrochim Acta 2004;49:965-78.
[9] Chatenet M, Micoud F, Roche I, Chainet E. Kinetics of borohydride oxidation and oxygen reduction in sodium hydroxide electrolyte: Part 1. BH4 electrooxidation on Au and Ag catalysts. Electrochim Acta 2006;51:5459–5467.
[10] Wei J, Wang X, Wang Y, Chen Q, Pei F, Wang Y. Investigation of carbonsupported Au hollow nanospheres as electrocatalyst for electrooxidation of sodium borohydride. Int J Hydrogen Energy 2009;34:3360-66.
[11] Ponce-de-LeYn C, Bavykin DV, Walsh FC. The oxidation of borohydride at titanate nanotube supported gold electrodes. Elec Comm 2006; 8:1655-1660.
[12] Nagle LC, Rohan JF. Ammonia borane oxidation at gold microelectrodes in alkaline solutions. J Electrochem Soc 2006;153:C773-6.
[13] Nagle LC,Rohan JF. Investigation of DMAB oxidation at a gold

microelectrode in base. Electrochemical and Solid-State Letters 2005;8(5): C77-80.
[14] Celikkan H, Sxahin M, Aksu ML, Vezirog˘lu TN. The investigation of the electro oxidation of sodium borohydride on various metal electrodes in aqueous basic solutions. Int J Hydrogen Energy 2007;32:588–93.
[15] Cao D, Gao Y, Wang G, Miao R, Liu Y. A direct NaBH4–H2O2 fuel cell using Ni foam supported Au nanoparticles as electrodes. Int J Hydrogen Energy 2010;35:807–813.
[16] Fu Pei , Ying Wangb, Xianyou Wanga,*, Peiying He a, Quanqi Chen a, Xingyan Wanga, Hong Wanga, Lanhua Yi a, Jia Guo. Performance of supported Au–Co alloy as the anode catalyst of direct borohydride-hydrogen peroxide fuel cell. Int J Hydrogen Energy 2010;35:8136-8142.
[17] Atwan MH, Northwood DO, Gyenge EL.Evaluation of colloidal Ag and Agalloys as anode electrocatalysts for direct borohydride fuel cells. Int J Hydrogen Energy 2007;32:3116-3125.
[18] Chatenet M, Molina-Concha M. B, Diard JP. First insights into the borohydride oxidation reaction mechanism on gold by impedance spectroscopy. Electrochim Acta 2009;54:1687–1693.
[19] Krishnan P, Yang T, Advani TH, Prasad AK. Rotating ring-disc electrode (RRDE) investigation of borohydride oxidation. J Power Sources 2008;182: 106–111.
[20] Chatenet M, Lima FHB, Ticianelli EA. Gold is not a Faradaic-Efficient Borohydride Oxidation Electrocatalyst: An Online Electrochemical Mass Spectrometry Study J Electrochem Soc 2010;B697.
[21] Finkelstein DA, Nicolas DM, Cohen JL, Abruna HD. Rotating Disk Electrode (RDE) Investigation of BH4 - and BH3OH- Electro-oxidation at Pt and Au: implications for BH4- fuel cells. J Phys Chem C 2009;113(45):19700-12.
[22] Molina Concha, Chatenet M. Direct oxidation of sodium borohydride on Pt, Ag and alloyed Pt–Ag electrodes in basic media Part II. Carbon-supported nanoparticles. Electrochim. Acta 2009;54:6130-6139
[23] Forty AJ. Corrosion micromorphology of noble metal alloys and depletion gilding. Nature 1979;282:597-8.
[24] Biener J, Hodge AM, Hayes JR, Volkert CA, Zepeda-Ruiz LA, Hamza AV, and Abraham FF. Size effects on the mechanical behaviour of nanoporous Au. Nano Lett 2006;6(10):2379-82.
[25] Sieradzki K and Karma A, Evolution of nanoporosity in dealloying Nature 2001 410:450-453.
[26] Pattricka G, van der Lingen E, Corti CW, Holliday RJ, Thompson DT. The potential for use of gold in automotive pollution control technologies: a short review. Top Catal 2004; 30: 273.
[27] Xu C, Su J, Xu X, Liu P, Zhao H, Tian F, Ding Y. Low Temperature CO Oxidation over Unsupported Nanoporous Gold. J Am Chem Soc 2007;129:42-3.
[28] Zielasek V, Jurgens B, Schulz C, Biener J, Biener M, Hamza AV and Baumer M. Nanoporous Gold Foams. Angew Chem Int Edn 2006;45:8241-4.
[29] Choudhary TV and Goodman DW, Catalytically active gold: The role of cluster morphology. Appl Catal A 2005;291:32-36.
[30] Zeis R, Lei T, Sieradzki K, Snyder J and Erlebacher J. Catalytic reduction of oxygen and hydrogen peroxide by nanoporous gold. J Catal 2008;253:132-8.
[31] Searson P and Ji C. Synthesis and Characterization of Nanoporous Gold

Nanowires. J Phys Chem B 2003;107:4494-9.
[32] Liu Z, Searson PC. Single Nanoporous Gold Nanowire Sensors. J Phys Chem B 2006; 110: 4318-4322.
[33] Sadik O, Xu H, Sargent A. Multielectron Transfer Mechanism of Dimethylamine Borane in Electroless Gold Deposition, J Electroanal Chem 2005;583:167-175.
[34] Molina Concha B, Chatenet M, El-Kissi N, Parrour G, Diard JP. Direct rotating ring-disk measurement of the sodium borohydride diffusion coefficient in sodium hydroxide solutions. Electrochim Acta 2009; 54:4426-4435.
[35] Molina Concha B, Chatenet M. Direct oxidation of sodium borohydride on Pt, Ag and alloyed Pt–Ag electrodes in basic media. Part I: Bulk electrodes Electrochim Acta 2009;54:6119-6129.
[36] Schneider A, Colmenares L, Seidel YE, Jusys Z, Wickman B, Kasemo B, Behm RJ. Transport effects in the oxygen reduction reaction on nanostructured, planar glassy carbon supported Pt/GC model electrodes. Phys. Chem. Chem. Phys. 2008;10:1931-1943.
[37] Zeis R, Mathur A, Fritz G, Lee J, Erlebacher J. Platinum-plated nanoporous gold: An efficient low Pt loading electrocatalyst for PEM fuel cells. J Power Sources 2007;165:65-72.

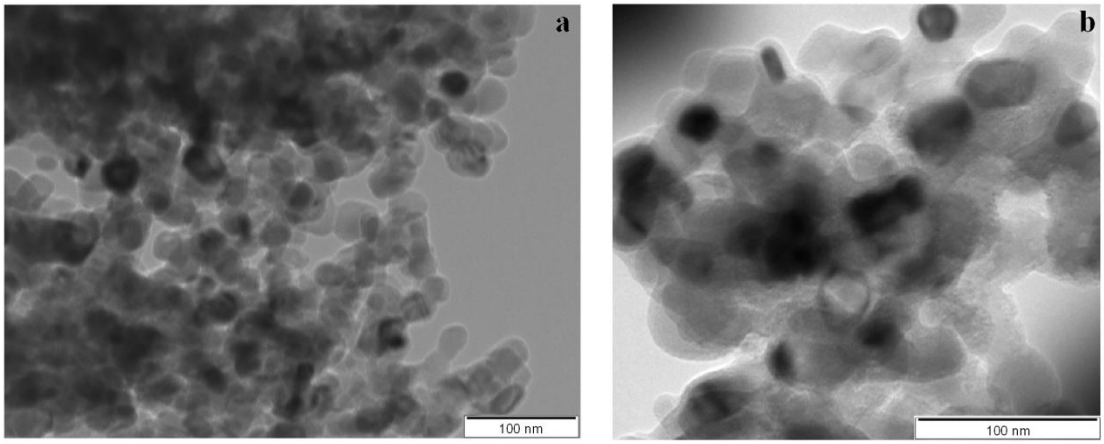


Fig 1.

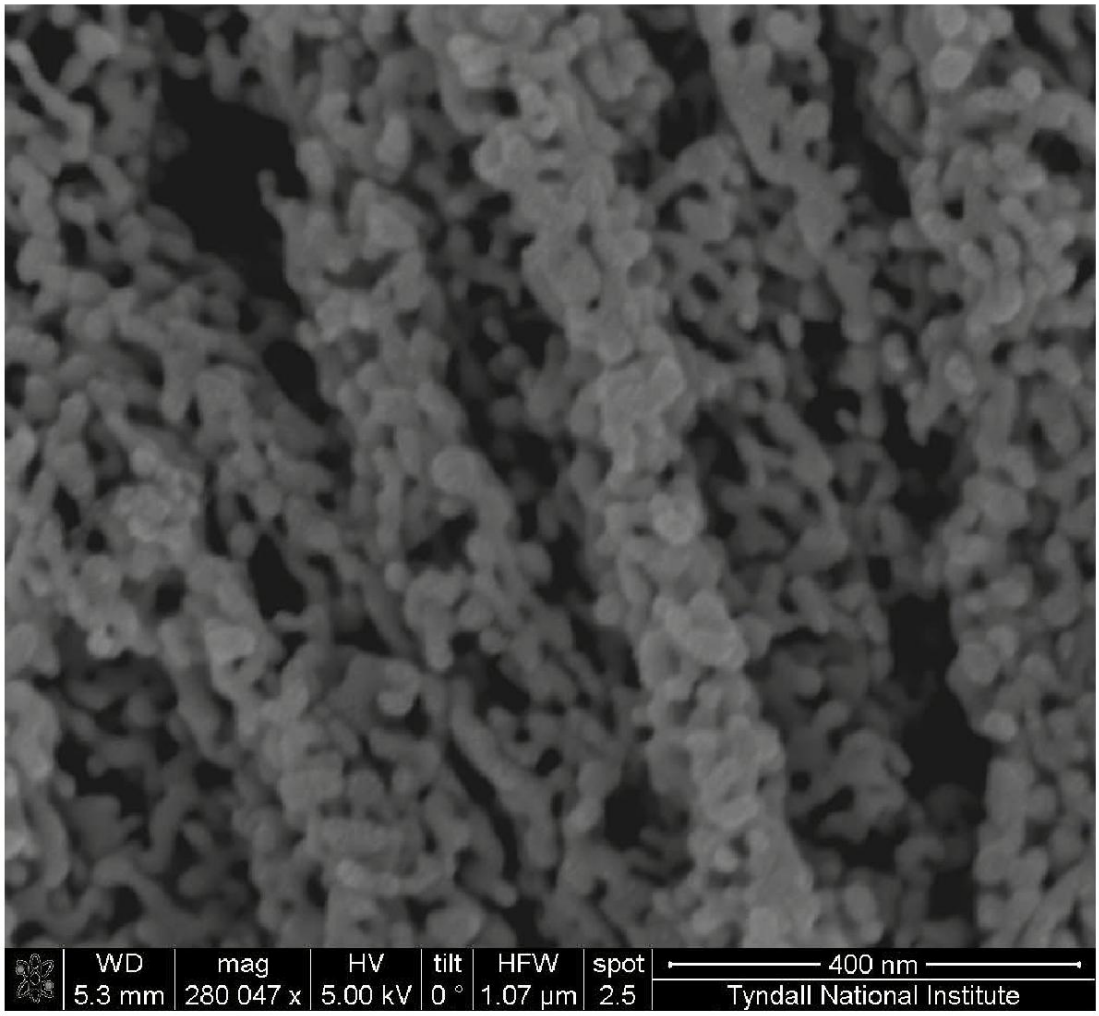

WD
5.3 mm
mag
280 047 x
HV
5.00 kV
tilt
0 °
HFW
1.07 µm
spot
2.5
400 nm
Tyndall National Institute

Fig. 2.

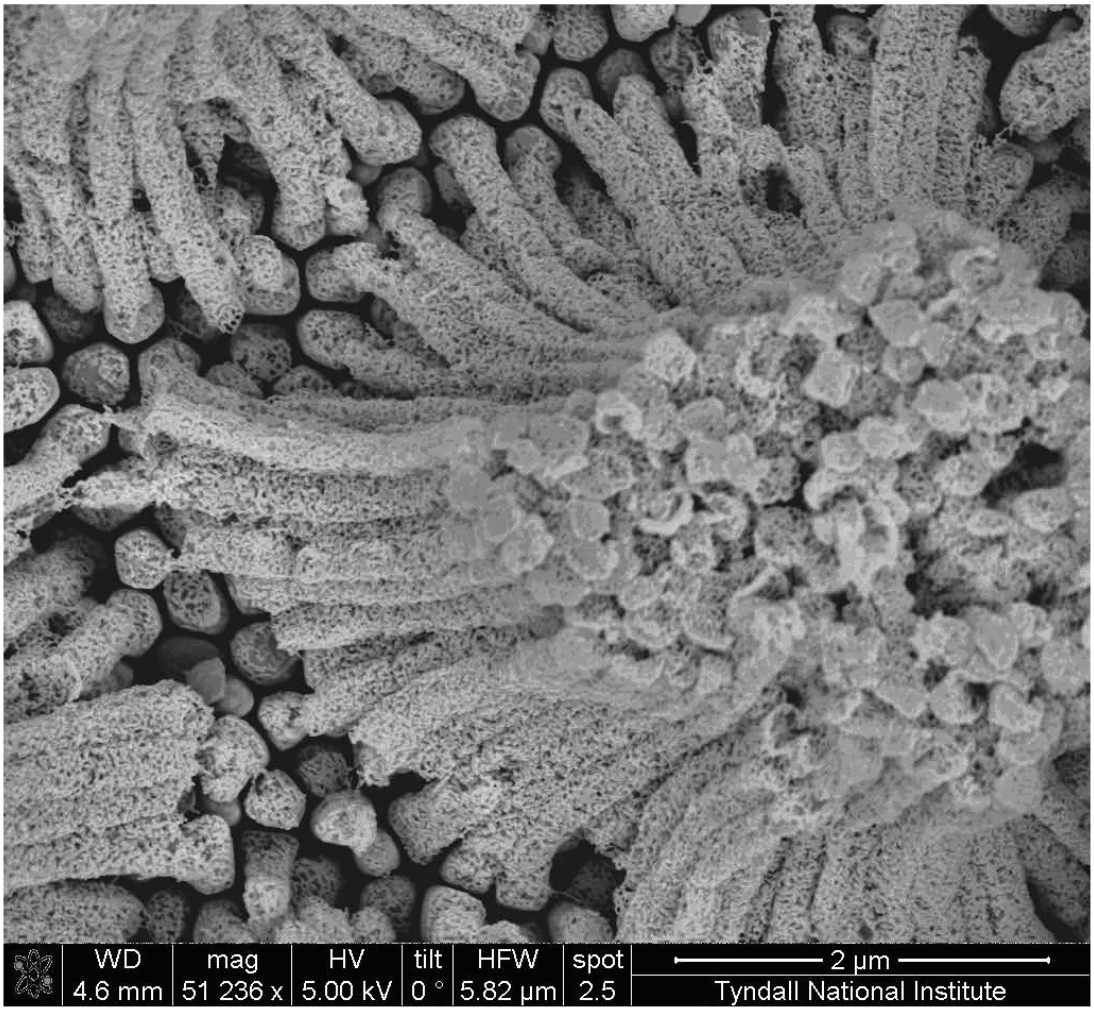

WD
4.6 mm
mag
51 236 x
HV
5.00 kV
tilt
0 °
HFW
5.82 µm
spot
2.5
2 µm
Tyndall National Institute

Fig. 3.

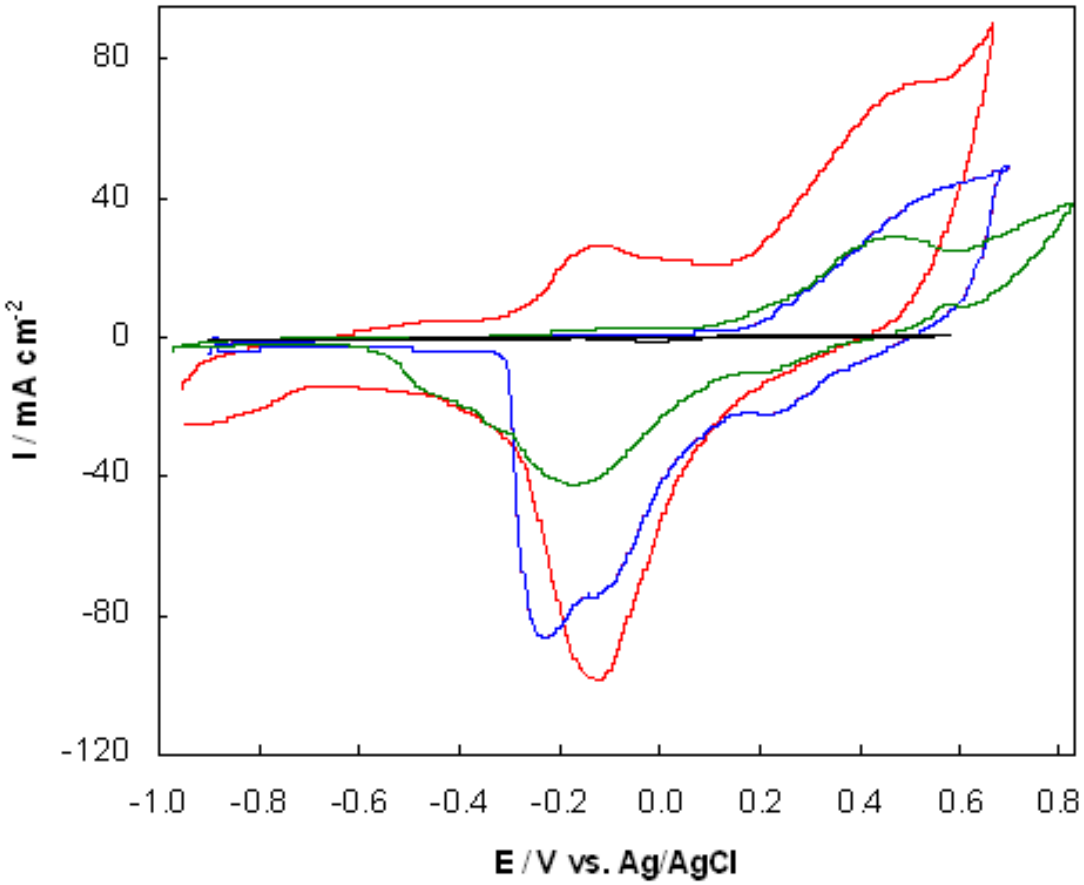


Fig. 4.

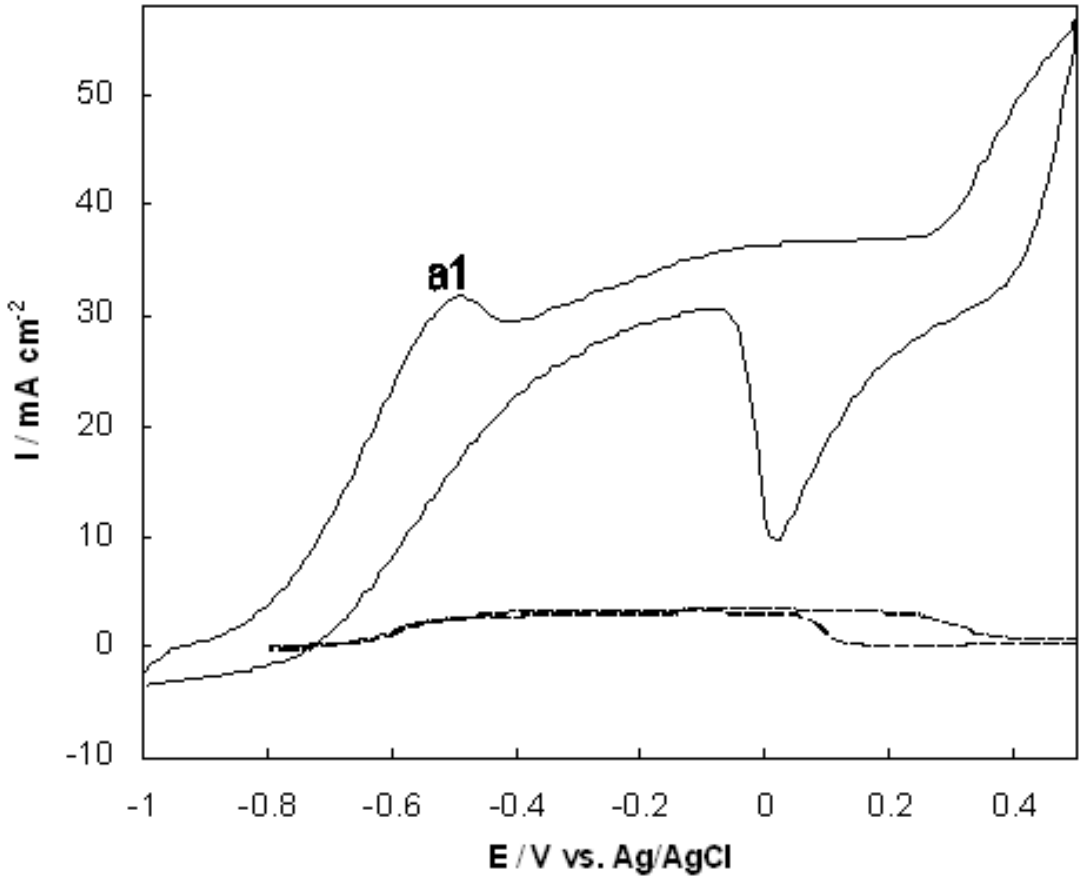


Fig.5.

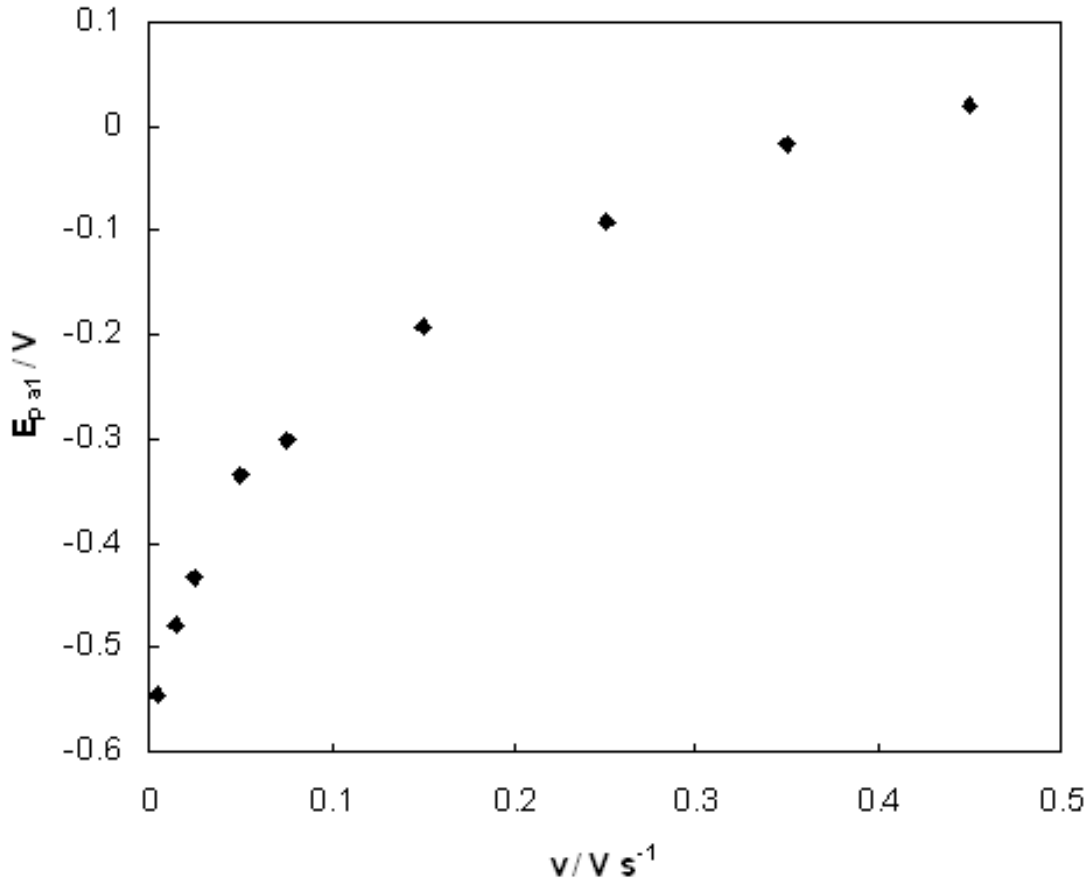


Fig.6.

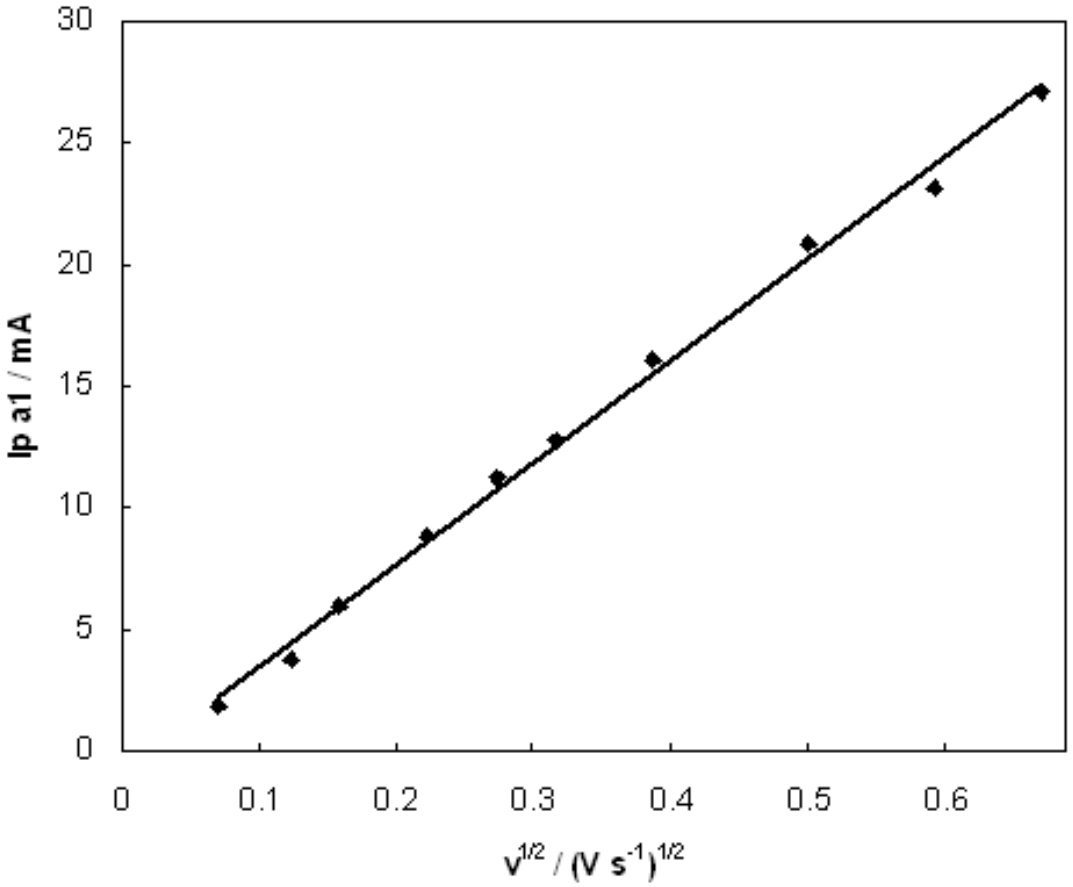

30
25
20
15
10
5
0
Ip a1 / mA
0
0.1
0.2
0.3
0.4
0.5
0.6
v^1/2 / (V s^-1)^1/2

Fig. 7.

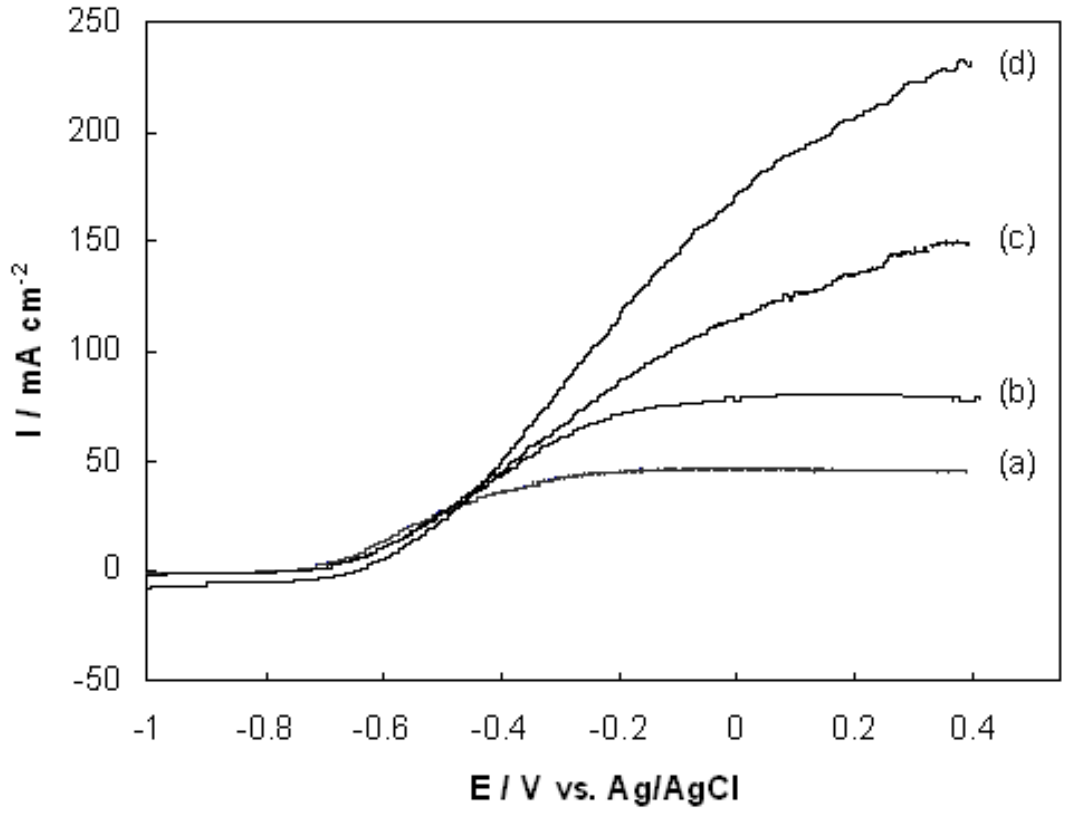

250
200
150
100
50
0
-50
I / mA cm^-2
(d)
(c)
(b)
(a)
-1
-0.8
-0.6
-0.4
-0.2
0
0.2
0.4
E / V vs. Ag/AgCl

Fig.8.

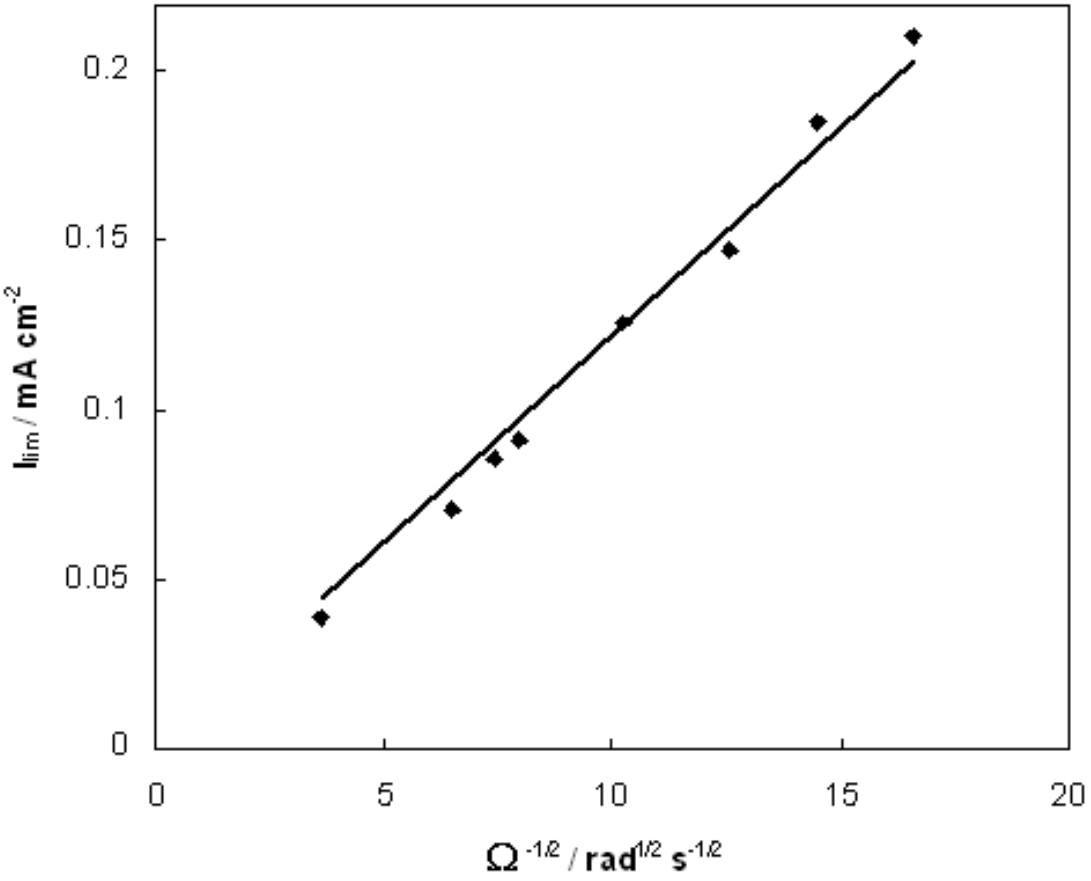


Fig.9.

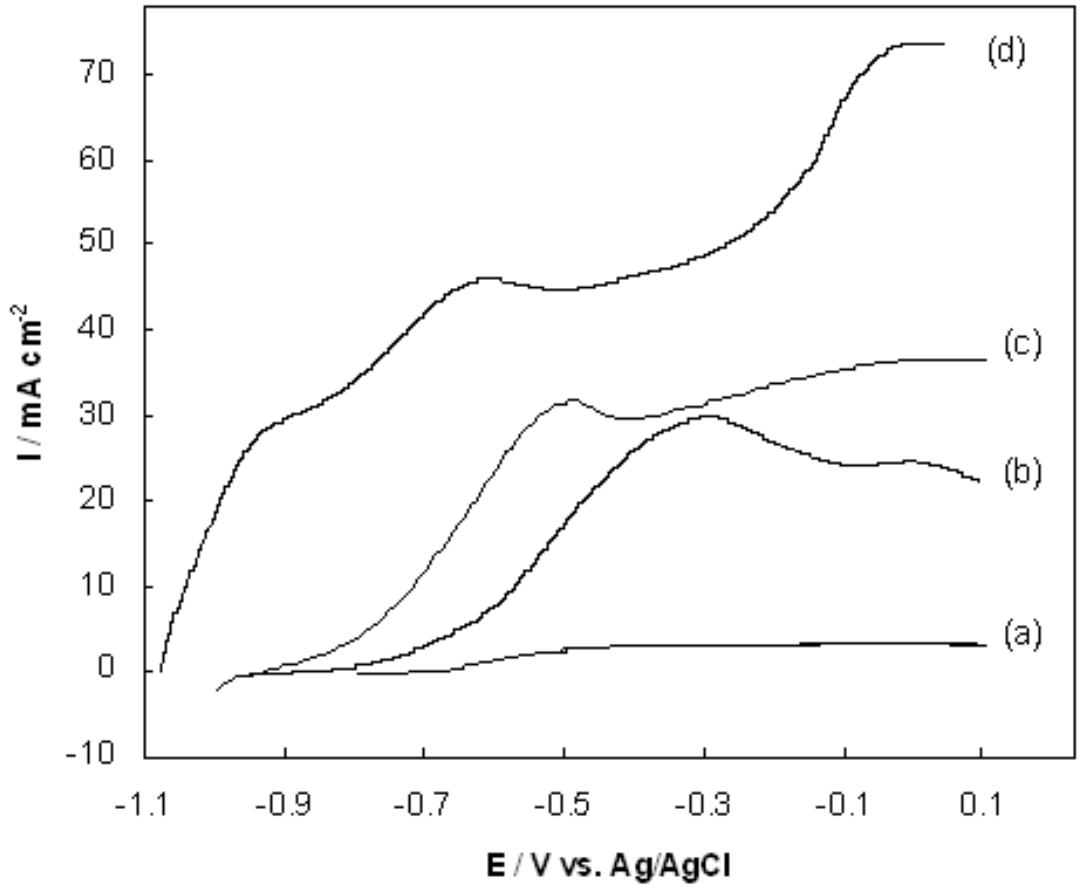

70
60
50
40
30
20
10
0
-10
I / mA cm-2
-1.1
-0.9
-0.7
-0.5
-0.3
-0.1
0.1
E / V vs. Ag/AgCl
(d)
(c)
(b)
(a)

Fig.10